European Radiology (2019) 29:6922–6929
https://doi.org/10.1007/s00330-019-06260-2

UROGENITAL

CT texture analysis in the differentiation of major renal cell carcinoma subtypes and correlation with Fuhrman grade

Yu Deng[1,2] · Erik Soule[3] · Aster Samuel[2] · Sakhi Shah[2] · Enming Cui[2,4] · Michael Asare-Sawiri[2,5] · Chandru Sundaram[6] · Chandana Lall[3] · Kumaresan Sandrasegaran[2,7]

Received: 14 February 2019 / Revised: 1 April 2019 / Accepted: 30 April 2019 / Published online: 24 May 2019

Abstract

Objective CT texture analysis (CTTA) using filtration-histogram–based parameters has been associated with tumor biologic correlates such as glucose metabolism, hypoxia, and tumor angiogenesis. We investigated the utility of these parameters for differentiation of clear cell from papillary renal cancers and prediction of Fuhrman grade.

Methods A retrospective study was performed by applying CTTA to pretreatment contrast-enhanced CT scans in 290 patients with 298 histopathologically confirmed renal cell cancers of clear cell and papillary types. The largest cross section of the tumor on portal venous phase axial CT was chosen to draw a region of interest. CTTA comprised of an initial filtration step to extract features of different sizes (fine, medium, coarse spatial scales) followed by texture quantification using histogram analysis.

Results A significant increase in entropy with fine and medium spatial filters was demonstrated in clear cell RCC ($p = 0.047$ and 0.033, respectively). Area under the ROC curve of entropy at fine and medium spatial filters was 0.804 and 0.841, respectively. An increased entropy value at coarse filter correlated with high Fuhrman grade tumors ($p = 0.01$). The other texture parameters were not found to be useful.

Conclusion Entropy, which is a quantitative measure of heterogeneity, is increased in clear cell renal cancers. High entropy is also associated with high-grade renal cancers. This parameter may be considered as a supplementary marker when determining aggressiveness of therapy.

Key points

- *CT texture analysis is easy to perform on contrast-enhanced CT.*
- *CT texture analysis may help to separate different types of renal cancers.*
- *CT texture analysis may enhance individualized treatment of renal cancers.*

Keywords Cone-beam computerized tomography · Image interpretation, computer-assisted · Clear cell renal cell carcinoma · Papillary renal cell carcinoma · Neoplasm grading

Abbreviations

ccRCC	Clear cell renal cell carcinoma
CTTA	Computerized tomography (CT) texture analysis
pRCC	Papillary renal cell carcinoma
RCC	Renal cell carcinoma
ROC curve	Receiver operating characteristic curve
SSF	Spatial scaling factor associated with CTTA

✉ Kumaresan Sandrasegaran
Sandrasegaran.kumaresan@mayo.edu

[1] Department of Radiology, The First Affiliated Hospital of Guangzhou Medical University, Guangzhou, China

[2] Department of Radiology, Indiana University School of Medicine, Indianapolis, IN, USA

[3] Department of Radiology, University of Florida College of Medicine, Jacksonville, FL, USA

[4] Department of Radiology, Jiangmen Central Hospital, Affiliated Jiangmen Hospital of Sun YAT-SEN University, Jiangmen, China

[5] Department of Oncology, Hope Regional Cancer Center, Panama, FL, USA

[6] Department of Urology, Indiana University School of Medicine, Indianapolis, IN, USA

[7] Department of Radiology, Mayo Clinic, 5777 E. Mayo Blvd, Phoenix, AZ 85054, USA

Introduction

Renal cell carcinoma (RCC) is among the ten most common cancers with an annual incidence of 295,000 and mortality of 134,000 worldwide [1, 2]. RCC encompasses a heterogeneous group of malignant entities with distinct pathology, biology, and treatment considerations [3]. The three most common subtypes are clear cell RCC (ccRCC, approximately 75%), papillary RCC (pRCC, 15%), and chromophobe RCC (5%) [4]. The Fuhrman system is widely used for grading RCC and has prognostic value, independent from tumor subtype. RCC is categorized as Fuhrman grade 1–4 based on nuclear characteristics (i.e., size, shape, and contents) [5]. An increasing interest has been drawn to the accurate imaging characterization of RCC given different prognostic and management considerations for each subtype and Fuhrman grade [6–11]. Although the degree of contrast enhancement may be valuable for differentiation, there is considerable overlap of imaging features between subtypes, including tumor size, attenuation/signal intensity, and growth pattern [12].

CT texture analysis (CTTA) has emerged as a promising technique for assessing tumor heterogeneity and as a biomarker in predicting treatment response and prognosis [13–15]. A few studies have looked at the value of CTTA in differentiating benign and malignant renal tumors [16, 17]. Two prior studies investigated the differentiation of clear cell and papillary renal cancers using CTTA [18, 19]. A small study ($n = 53$) showed that machine learning–based CTTA was able to predict Fuhrman grade of renal cancers [20]. However, to our knowledge, no study has evaluated CTTA for its ability to both differentiate ccRCC from pRCC and predict the pathological grade of these tumors. The purpose of this study is to investigate CTTA parameters in the differentiation ccRCC from pRCC and to attempt prediction of the Fuhrman grade of RCC, based on a large cohort.

Materials and methods

Patients

This HIPAA-compliant retrospective study was approved by the Institutional Review Board with a waiver of informed consent. The pathology database was queried to find all the cases with histopathologic confirmation of ccRCC or pRCC between January 2007 and December 2014. Only cases with available contrast-enhanced CT studies before treatment were included. The inclusion and exclusion criteria were selected to minimize confounding variables (Fig. 1).

CT examination

All contrast-enhanced CT scans were performed on multislice CT systems (Philips Medical Systems), using similar protocols: 120 kVp, 180–450 mA with automatic tube current modulation, matrix of 512, field of view of 380–500 mm, and 4- or 5-mm reconstructed section thickness. Intravenous injection of 120 mL of 370 mg of iodine/mL of iopamidol (Isovue 370, Bracco Diagnostics) was delivered at 3 mL/s. The portal venous phase was obtained 75 s after commencement of contrast agent administration.

CT texture analysis

CT images were reviewed, and the maximum tumor diameter was recorded at a picture archiving and communications system (PACS) workstation (Synapse, Fujifilm Medical Systems) by a radiologist with 15 years of experience in body imaging (YD), blinded to pathology. The axial-enhanced CT image of the largest tumor cross section was identified, anonymized, and exported to a Digital Imaging and Communications in Medicine (DICOM) file. The DICOM files were uploaded to a cloud server with the TexRAD CTTA software (version 3.9, TexRAD Ltd.). A region of interest (ROI) was drawn to include the entire tumor (Fig. 2). The solid lesion algorithm was implemented which included only pixels above – 50 HU within the ROI using "threshold" as padding (erosion scale = 0) for reducing edge artifact.

CTTA methodology using the filtration-histogram technique has been described elsewhere [13, 21–23]. Once ROIs are obtained, the CTTA software modifies the pixel data using several Laplacian spatial scaling factors (SSF), which extracts and enhances features of different sizes (mm) ranging from fine (SSF = 2 mm), medium (SSF = 4 mm), and coarse (SSF = 6 mm) texture scales. A fine filter tends to enhance tissue parenchymal features, while medium to coarse filters enhance vascular features [24]. The filtration step derives filtered maps, which are quantified to yield four parameters by histogram and statistical analysis. These parameters were mean value of positive pixels (average brightness considering only the positive pixel values), entropy (heterogeneity of pixel intensities), kurtosis (peakedness or sharpness of the pixel distribution), and skewness (asymmetry of pixel distribution). The mathematical process of calculating these parameters has been previously described [15, 25, 26].

Reference standard

The prospective histopathological reports were used as the reference standard. These were read by fellowship-trained histopathologists specialized in renal diseases. The Fuhrman grading was performed as per well-established guidelines [27]. As per multiple prior imaging and clinical studies

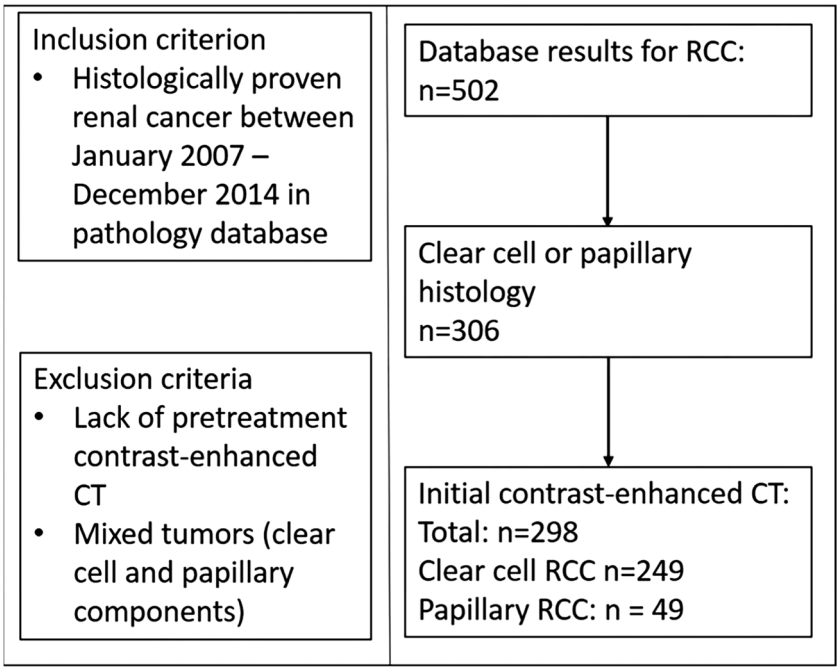

Fig. 1 Inclusion and exclusion criteria for study cohort

assessing outcome of renal cancers, we separated high-grade (Fuhrman 3, 4) from low-grade (Fuhrman 1, 2) cancers [20, 28–30].

Statistical analysis

The age of the patient and the size of the ccRCC and pRCC tumors were compared using two independent samples *t* test. The gender and Fuhrman grade between ccRCC and pRCC were compared using the chi-square test. A binary logistic regression analysis was performed to quantify any correlation between the CTTA parameters and the tumor size or histology. Receiver operating characteristic (ROC) analyses were used to assess the performance of CTTA parameters in the differentiation of subtypes of RCC. A multinomial logistic regression analysis was performed to correlate the CTTA parameters with Fuhrman grade. Statistical analysis was performed by using IBM SPSS Statistics for Windows, version 24.0 (IBM Corp.). Holm-Bonferroni correction of p values for multiple testing bias [31] was performed. A corrected $p < 0.05$ was deemed statistically significant.

Results

Demographics

The final cohort consisted of 244 patients with 249 ccRCC lesions (5 patients had two lesions) and 46 patients with 49 pRCC lesions (3 patients had two lesions). Epidemiological and clinical differences between the two groups of patients are given in Table 1. The only significant difference noted was that pRCC patients were more likely to be males than ccRCC patients ($p = 0.01$).

Comparison of CTTA parameters between ccRCC and pRCC

There was no significant difference in tumor sizes between the ccRCC and pRCC groups ($p = 0.94$). The CTTA parameters for ccRCC and pRCC and their value in differentiating the two entities are given in Table 2. The box and whisker plot of entropy values of renal cancers at medium spatial filter is given in Fig. 3. Entropy with fine and medium spatial filters of ccRCC was significantly higher than that of pRCC ($p =$ 0.047 and 0.033, respectively).

Area under the ROC curves (AUC) of entropy at fine, medium, and coarse spatial filters were 0.804 with a 95% confidence interval of 0.755–0.848, 0.841 (0.803–0.888), and 0.822 (0.774–0.864), respectively (Fig. 4). Entropy greater than 5.34 at medium spatial filter had sensitivity and specificity of 77.5% and 83.7%, respectively, for diagnosing ccRCC.

Correlation between CTTA parameters and Fuhrman grade

High Fuhrman grade (3 and 4) cancers were associated with larger tumor diameter ($p < 0.001$) and a high entropy value ($p = 0.01$) with a coarse filter (SSF6). The other parameters were not significantly associated with high Fuhrman grade.

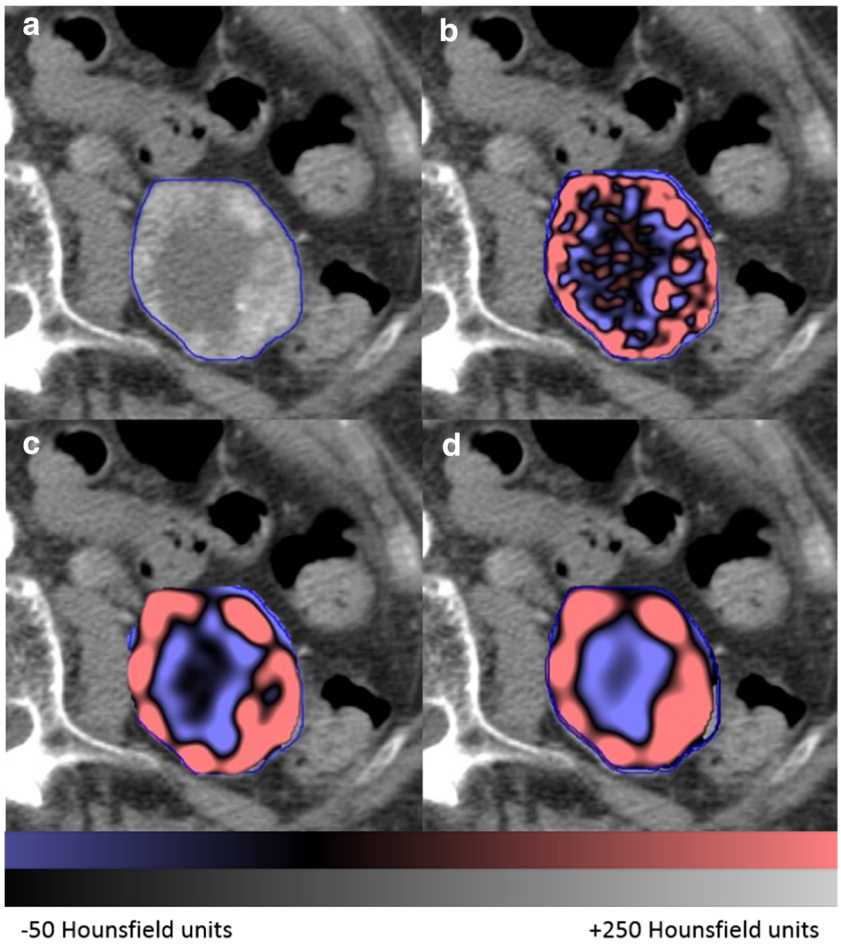

Fig. 2 CT texture analysis of ccRCC. **a** Delineation of tumor (blue line). **b–d** Color texture overlays of tumor outlined by ROI at fine (**b**), medium (**c**), and coarse (**d**) spatial filters. These images undergo pixel-by-pixel histogram analysis to yield CTTA parameters. When a fine spatial filter is applied, the internal structure of the tumor can be clearly seen

Discussion

CTTA has demonstrated promising diagnostic and prognostic capabilities for evaluation of malignancies and other disease processes, especially in the pulmonary, gastrointestinal, and genitourinary systems [32–34]. Further refinement and standardization of protocols and parameters may allow CTTA to be implemented in clinical practice. For example, in heterogeneous tumors such as RCC, a percutaneous biopsy of one region of the tumor may underestimate the overall tumor grade. Performing CTTA in this circumstance could function as a "failsafe," triggering additional investigation and mitigating sampling bias. CTTA could also potentially spare biopsy or resection for poor surgical candidates. If the lesion appears unlikely to cause short-term morbidity and mortality, a multidisciplinary "wait and watch" approach may be selected.

The current paradigm of RCC imaging interpretation is based on a visual process which includes assessment of the shape, margin, as well as degree and heterogeneity of enhancement. These subjective methods do not adequately address discrepancies in the cellularity, angiogenesis, matrix, and areas of necrosis between different tumor subtypes (i.e., inter-tumoral heterogeneity) [35]. Texture analysis is an image processing technique that can extract texture information in a quantitative manner, allowing for mathematical detection of changes in pixel intensity which may be visually imperceptible. This study explores the usefulness of texture analysis for the differentiation of ccRCC from pRCC and for predicting Fuhrman grade.

Prior studies have shown that ccRCC enhance substantially more than pRCC, particularly in the corticomedullary phase of enhancement [9, 10, 36–39]. Sensitivity and specificity of contrast-enhanced CT in distinguishing ccRCC and pRCC have been reported to vary from 70 to 98 and 62–92, respectively [9, 10, 12, 39]. Some studies have suggested that on the whole ccRCC are subjectively more heterogenous than pRCC [40]. However, when heterogeneity was assigned a three-point score, there was substantial overlap in the scores of ccRCC and pRCC [41]. In another study, 84% of ccRCC and 74% of pRCC subjectively showed heterogenous enhancement [12]. Thus, an objective score of heterogeneity, such as entropy seen in CTTA, may help increase specificity in some cases to distinguish ccRCC from pRCC. In such cases, CTTA may obviate need for additional imaging tests, such as MRI.

Among CTTA parameters, entropy was seen to be the best predictor for differentiation of ccRCC from pRCC. Entropy

Table 1 Patient characteristics

	Clear cell RCC ($n = 249$)	Papillary RCC ($n = 49$)	p
Age	60.1 (18–93 years)	62.7 (34–75 years)	0.18
Gender	M:F = 147:102	M:F = 38:11	0.01
Fuhrman grade (low/high)	173/76	30/19	0.26
AJCC stage (1/2/3/4)	187/15/40/4*	41/5/3/0	0.12
Tumor size in cm: mean (SD)	4.0 (2.6)	4.1 (2.7)	0.94

Except where indicated, data are numbers of patients

AJCC, American Joint Committee on Cancer staging classification: 7th edition

*No staging available in 3 patients

represents the randomness or irregularity of gray-value distribution, and heterogeneous tumors tend to have greater entropy [42]. In accordance with previous studies, ccRCC demonstrates higher entropy compared to pRCC, signifying increased intra-tumoral heterogeneity [41]. Entropy greater than 5.34 at medium spatial filter (SSF4) has sensitivity and specificity of 74% and 88%, respectively, to distinguish of ccRCC from pRCC, a significant improvement in specificity when compared to standard techniques. Chen et al also demonstrated increased entropy of ccRCC compared to pRCC (increased standard deviation and interquartile range), most apparent in the arterial phase of the CT examination [19]. Lubner et al found that entropy higher than 4.86 was the best predictor of ccRCC [18]. In addition, they found that high mean of positive pixels was associated with ccRCC. We did not find this to be the case. There are a few potential reasons for the differences between our paper and that of Lubner et al. Our cohort is much larger. The Holms correction for multiple testing bias that we used is thought to be more stringent than the Bonferroni correction [31] used in the paper of Lubner et al.

The heterogeneity of RCC as elucidated by CTTA also demonstrates a statistically significant association with Fuhrman grade in this study. High entropy at coarse filter correlates with high Fuhrman grade ($p = 0.05$). Various CTTA parameters have demonstrated efficacy for grading malignancy in multiple organs, highlighting the need for future research in this field. In a study of 44 patients with gliomas, the coarse texture entropy and uniformity are found useful in distinguishing between low- and high-grade tumors [43]. In addition to higher entropy, higher standard deviation, higher kurtosis, and positive skewness are postulated to represent increased intra-tumoral heterogeneity and portend poorer prognosis [44, 45]. Recent studies correlate imaging features to Fuhrman grade and find that intra-tumoral necrosis was a strong predictor of aggressive histology [46, 47]. Visually imperceptible intra-tumoral necrosis, however, may result in underestimation of tumor heterogeneity and aggressiveness. In a study of differentiation between lipid-poor angiomyolipoma and RCC based on unenhanced CTTA, Hodgdon et al find that visual analysis was less accurate than textural analysis [48]. In

Table 2 CTTA parameters in differentiating ccRCC from pRCC

Spatial filter	CTTA parameter	ccRCC*	pRCC*	p value**
Fine (SSF 2)	Entropy	8.3 (14.8)	− 4.9 (21.4)	0.047
	Mean pos.***	5.6 (0.3)	5.22 (0.35)	0.907
	Skewness	0.01 (0.48)	− 0.07 (0.51)	0.113
	Kurtosis	0.96 (4.27)	1.17 (2.34)	0.114
Medium (SSF 4)	Entropy	14.3 (28.1)	− 10.1 (29.0)	0.033
	Mean pos. ***	5.6 (0.33)	5.1 (0.3)	0.076
	Skewness	− 0.01 (0.43)	0.15 (0.61)	0.524
	Kurtosis	0.18 (1.23)	1.90 (4.64)	0.085
Coarse (SSF 6)	Entropy	17.8 (37,9)	− 13.3 (30.1)	0.053
	Mean pos. ***	5.54 (0.36)	5.1 (0.38)	0.055
	Skewness	− 0.09 (0.46)	0.18 (0.72)	0.634
	Kurtosis	− 0.05 (0.86)	1.63 (3.76)	0.260

*Mean (standard deviation) of CTTA parameter values

**p values after Holm correction

***Mean value of positive pixels

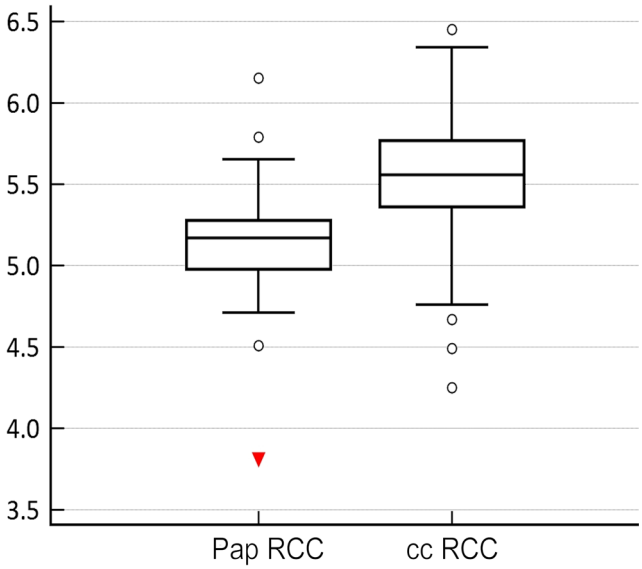

Fig. 3 Box and whisker plot of entropy values for papillary (pRCC) and clear cell (ccRCC) renal cancers at medium spatial scaling filter (SSF = 4). Pap RCC, papillary-type renal cell carcinoma; ccRCC, clear cell–type renal cell carcinoma. Boxes represent interquartile range. Central line in the box is the median value. Whiskers represent range of all values. Small circles and triangles refer to outliers. Note that the boxes of the two groups of RCC do not overlap

this context, CTTA may be more objective than visual analysis to assess heterogeneity inside an RCC. Consistent with previous studies, tumor size also demonstrates significant correlation with Fuhrman grade [49, 50]. Therefore, increased intratumoral heterogeneity (entropy) and large tumor size are risk factors for high-grade malignancy.

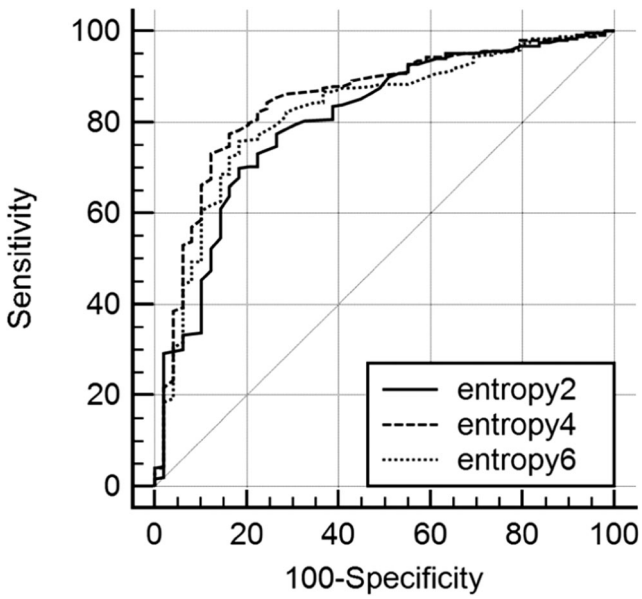

Fig. 4 ROC curves plotting sensitivity (y-axis) and 1-specificity (x-axis) of entropy at different spatial filters in differentiating ccRCC from pRCC. Entropy 2, entropy at fine spatial filter (SSF = 2 mm); entropy 4, entropy at medium spatial filter (SSF = 4 mm); entropy 6, entropy at coarse spatial filter (SSF = 6 mm). Area under ROC curves (AUC) are given in the text

We are aware of limitations of our study. Our study was retrospective. We had only one CTTA reviewer in this study. However, prior CTTA studies have shown good to excellent interobserver agreement [48, 51–54]. We used a single axial slice of tumor to assess CTTA, rather than using a three-dimensional approach. The latter would have been time consuming to do in large cohort. It has been shown that two-dimensional texture analysis gives adequate results, though multi-slice volume analysis may be more representative of tumor [55]. Selection bias toward high-grade, larger tumors may have been introduced due to the need for histopathologic confirmation in the study design. Smaller tumors, especially in older patients, may not necessarily undergo surgical excision. The prognostic ability of Fuhrman tumor grading for pRCC remains unclear currently due to conflicting evidence [56, 57]. Nevertheless, in routine urological practice, Fuhrman grading continues to be used. Finally, only two of the CTTA parameters tested achieved statistical significance for discrimination of ccRCC from pRCC, with p values that approached the cutoff of less than 0.05. This was mainly due to the robust post hoc Holm correction that was employed to reduce type I errors [31].

Establishing a more sophisticated and automatic tumor border tracking method is a promising future direction for this research to enable full evaluation of the volumetric heterogeneity of the tumor. We did not perform high-order statistics such as gray-level co-occurrence matrix (GLCM), gray-level run-length (GLRL), gray-level gradient matrix (GLGM), and Laws' features [16, 35]. The first-order texture analysis performed in this study, however, was easy to implement and spatially invariant. Several studies prove that first-order parameters correlate to underlying physiological changes. The correlation between higher order texture analysis–derived parameters with pathophysiological changes remains unknown, although a recent study shows the diagnostic performance of first-order CCTA is more accurate than higher order CTTA in the differentiation of renal tumors [16].

In conclusion, CTTA is a promising modality for evaluation of renal tumors. CTTA may have utility for discrimination of tumor subtype, and for prediction of aggressive phenotypes. Entropy at fine and medium spatial scaling filters was able to differentiate ccRCC from pRCC with high specificity and sensitivity. Large tumor size and increased entropy correlate with high Fuhrman grade.

Funding The authors state that this work has not received any funding.

Compliance with ethical standards

Guarantor The scientific guarantor of this publication is Kumaresan Sandrasegaran, M.D.

Conflict of interest The authors of this manuscript declare no relationships with any companies whose products or services may be related to the subject matter of the article.

Statistics and biometry No complex statistical methods were necessary for this paper.

Informed consent Written informed consent was waived by the Institutional Review Board.

Ethical approval Institutional Review Board approval was obtained.

Methodology
- Retrospective
- Case-control study
- Performed at one institution

References

1. Torre LA, Bray F, Siegel RL, Ferlay J, Lortet-Tieulent J, Jemal A (2015) Global cancer statistics, 2012. CA Cancer J Clin 65:87–108
2. Global Burden of Disease Cancer Collaboration, Fitzmaurice C, Dicker D et al (2015) The global burden of cancer 2013. JAMA Oncol 1:505–527
3. Moch H, Cubilla AL, Humphrey PA, Reuter VE, Ulbright TM (2016) The 2016 WHO classification of tumours of the urinary system and male genital organs-part a: renal, penile, and testicular tumours. Eur Urol 70:93–105
4. Hsieh JJ, Purdue MP, Signoretti S et al (2017) Renal cell carcinoma. Nat Rev Dis Primers 3:17009
5. Fuhrman SA, Lasky LC, Limas C (1982) Prognostic significance of morphologic parameters in renal cell carcinoma. Am J Surg Pathol 6:655–663
6. Young JR, Coy H, Kim HJ et al (2017) Performance of relative enhancement on multiphasic MRI for the differentiation of clear cell renal cell carcinoma (RCC) from papillary and chromophobe RCC subtypes and oncocytoma. AJR Am J Roentgenol 208:812–819
7. Mytsyk Y, Dutka I, Borys Y et al (2017) Renal cell carcinoma: applicability of the apparent coefficient of the diffusion-weighted estimated by MRI for improving their differential diagnosis, histologic subtyping, and differentiation grade. Int Urol Nephrol 49:215–224
8. Kasoji SK, Chang EH, Mullin LB, Chong WK, Rathmell WK, Dayton PA (2017) A pilot clinical study in characterization of malignant renal-cell carcinoma subtype with contrast-enhanced ultrasound. Ultrason Imaging 39:126–136
9. Young JR, Margolis D, Sauk S, Pantuck AJ, Sayre J, Raman SS (2013) Clear cell renal cell carcinoma: discrimination from other renal cell carcinoma subtypes and oncocytoma at multiphasic multidetector CT. Radiology 267:444–453
10. Pierorazio PM, Hyams ES, Tsai S et al (2013) Multiphasic enhancement patterns of small renal masses (</=4 cm) on preoperative computed tomography: utility for distinguishing subtypes of renal cell carcinoma, angiomyolipoma, and oncocytoma. Urology 81:1265–1271
11. Cheville JC, Lohse CM, Zincke H, Weaver AL, Blute ML (2003) Comparisons of outcome and prognostic features among histologic subtypes of renal cell carcinoma. Am J Surg Pathol 27:612–624
12. Kim JK, Kim TK, Ahn HJ, Kim CS, Kim KR, Cho KS (2002) Differentiation of subtypes of renal cell carcinoma on helical CT scans. AJR Am J Roentgenol 178:1499–1506
13. Miles KA, Ganeshan B, Hayball MP (2013) CT texture analysis using the filtration-histogram method: what do the measurements mean? Cancer Imaging 13:400–406
14. Ganeshan B, Goh V, Mandeville HC, Ng QS, Hoskin PJ, Miles KA (2013) Non-small cell lung cancer: histopathologic correlates for texture parameters at CT. Radiology 266:326–336
15. Goh V, Ganeshan B, Nathan P, Juttla JK, Vinayan A, Miles KA (2011) Assessment of response to tyrosine kinase inhibitors in metastatic renal cell cancer: CT texture as a predictive biomarker. Radiology 261:165–171
16. Yu H, Scalera J, Khalid M et al (2017) Texture analysis as a radiomic marker for differentiating renal tumors. Abdom Radiol (NY). https://doi.org/10.1007/s00261-017-1144-1
17. Raman SP, Chen Y, Schroeder JL, Huang P, Fishman EK (2014) CT texture analysis of renal masses: pilot study using random forest classification for prediction of pathology. Acad Radiol 21:1587–1596
18. Lubner MG, Stabo N, Abel EJ, Del Rio AM, Pickhardt PJ (2016) CT textural analysis of large primary renal cell carcinomas: pretreatment tumor heterogeneity correlates with histologic findings and clinical outcomes. AJR Am J Roentgenol 207:96–105
19. Chen F, Huhdanpaa H, Desai B et al (2015) Whole lesion quantitative CT evaluation of renal cell carcinoma: differentiation of clear cell from papillary renal cell carcinoma. Springerplus 4:66
20. Bektas CT, Kocak B, Yardimci AH et al (2018) Clear cell renal cell carcinoma: machine learning-based quantitative computed tomography texture analysis for prediction of Fuhrman nuclear grade. Eur Radiol. https://doi.org/10.1007/s00330-018-5698-2
21. Ng F, Ganeshan B, Kozarski R, Miles KA, Goh V (2013) Assessment of primary colorectal cancer heterogeneity by using whole-tumor texture analysis: contrast-enhanced CT texture as a biomarker of 5-year survival. Radiology 266:177–184
22. Ganeshan B, Miles KA (2013) Quantifying tumour heterogeneity with CT. Cancer Imaging 13:140–149
23. Ganeshan B, Abaleke S, Young RC, Chatwin CR, Miles KA (2010) Texture analysis of non-small cell lung cancer on unenhanced computed tomography: initial evidence for a relationship with tumour glucose metabolism and stage. Cancer Imaging 10:137–143
24. Yip C, Landau D, Kozarski R et al (2014) Primary esophageal cancer: heterogeneity as potential prognostic biomarker in patients treated with definitive chemotherapy and radiation therapy. Radiology 270:141–148
25. Ganeshan B, Skogen K, Pressney I, Coutroubis D, Miles K (2012) Tumour heterogeneity in oesophageal cancer assessed by CT texture analysis: preliminary evidence of an association with tumour metabolism, stage, and survival. Clin Radiol 67:157–164
26. Sasaguri K, Takahashi N, Gomez-Cardona D et al (2015) Small (< 4 cm) renal mass: differentiation of oncocytoma from renal cell carcinoma on biphasic contrast-enhanced CT. AJR Am J Roentgenol 205:999–1007
27. Delahunt B, Eble JN, Egevad L, Samaratunga H (2019) Grading of renal cell carcinoma. Histopathology 74:4–17
28. Ding J, Xing Z, Jiang Z et al (2018) CT-based radiomic model predicts high grade of clear cell renal cell carcinoma. Eur J Radiol 103:51–56
29. Zhang X, Wang Y, Yang L et al (2018) Delayed enhancement of the peritumoural cortex in clear cell renal cell carcinoma: correlation with Fuhrman grade. Clin Radiol 73:982 e981-982 e987
30. Gu L, Li H, Wang Z et al (2018) A systematic review and meta-analysis of clinicopathologic factors linked to oncologic outcomes for renal cell carcinoma with tumor thrombus treated by radical nephrectomy with thrombectomy. Cancer Treat Rev 69:112–120
31. Aickin M, Gensler H (1996) Adjusting for multiple testing when reporting research results: the Bonferroni vs Holm methods. Am J Public Health 86:726–728
32. Lubner MG, Smith AD, Sandrasegaran K, Sahani DV, Pickhardt PJ (2017) CT texture analysis: definitions, applications, biologic correlates, and challenges. Radiographics 37:1483–1503

33. Sandrasegaran K, Lin Y, Asare-Sawiri M, Taiyini T, Tann M (2019) CT texture analysis of pancreatic cancer. Eur Radiol 29:1067–1073
34. Zhang GM, Sun H, Shi B, Jin ZY, Xue HD (2017) Quantitative CT texture analysis for evaluating histologic grade of urothelial carcinoma. Abdom Radiol (NY) 42:561–568
35. Davnall F, Yip CS, Ljungqvist G et al (2012) Assessment of tumor heterogeneity: an emerging imaging tool for clinical practice? Insights Imaging 3:573–589
36. Veloso Gomes F, Matos AP, Palas J et al (2015) Renal cell carcinoma subtype differentiation using single-phase corticomedullary contrast-enhanced CT. Clin Imaging 39:273–277
37. Sheir KZ, El-Azab M, Mosbah A, El-Baz M, Shaaban AA (2005) Differentiation of renal cell carcinoma subtypes by multislice computerized tomography. J Urol 174:451–455 discussion 455
38. Shebel HM, Elsayes KM, Sheir KZ et al (2011) Quantitative enhancement washout analysis of solid cortical renal masses using multidetector computed tomography. J Comput Assist Tomogr 35: 337–342
39. Ruppert-Kohlmayr AJ, Uggowitzer M, Meissnitzer T, Ruppert G (2004) Differentiation of renal clear cell carcinoma and renal papillary carcinoma using quantitative CT enhancement parameters. AJR Am J Roentgenol 183:1387–1391
40. Zhang J, Lefkowitz RA, Ishill NM et al (2007) Solid renal cortical tumors: differentiation with CT. Radiology 244:494–504
41. Leng S, Takahashi N, Gomez Cardona D et al (2017) Subjective and objective heterogeneity scores for differentiating small renal masses using contrast-enhanced CT. Abdom Radiol (NY) 42: 1485–1492
42. Yip C, Davnall F, Kozarski R et al (2015) Assessment of changes in tumor heterogeneity following neoadjuvant chemotherapy in primary esophageal cancer. Dis Esophagus 28:172–179
43. Skogen K GB, Good T, Critchley G, Miles KA (2011) Imaging heterogeneity in gliomas using texture analysis. Cancer Imaging 11 Spec No A:A113
44. Castellano G, Bonilha L, Li LM, Cendes F (2004) Texture analysis of medical images. Clin Radiol 59:1061–1069
45. Yang Z, Tang LH, Klimstra DS (2011) Effect of tumor heterogeneity on the assessment of Ki67 labeling index in well-differentiated neuroendocrine tumors metastatic to the liver: implications for prognostic stratification. Am J Surg Pathol 35:853–860
46. Oh S, Sung DJ, Yang KS et al (2017) Correlation of CT imaging features and tumor size with Fuhrman grade of clear cell renal cell carcinoma. Acta Radiol 58:376–384
47. Beddy P, Genega EM, Ngo L et al (2014) Tumor necrosis on magnetic resonance imaging correlates with aggressive histology and disease progression in clear cell renal cell carcinoma. Clin Genitourin Cancer 12:55–62
48. Hodgdon T, McInnes MD, Schieda N, Flood TA, Lamb L, Thornhill RE (2015) Can quantitative CT texture analysis be used to differentiate fat-poor renal angiomyolipoma from renal cell carcinoma on unenhanced CT images? Radiology 276:787–796
49. Thompson RH, Kurta JM, Kaag M et al (2009) Tumor size is associated with malignant potential in renal cell carcinoma cases. J Urol 181:2033–2036
50. Turun S, Banghua L, Zheng S, Wei Q (2012) Is tumor size a reliable predictor of histopathological characteristics of renal cell carcinoma? Urol Ann 4:24–28
51. Hayano K, Tian F, Kambadakone AR et al (2015) Texture analysis of non-contrast-enhanced computed tomography for assessing angiogenesis and survival of soft tissue sarcoma. J Comput Assist Tomogr 39:607–612
52. Schieda N, Thornhill RE, Al-Subhi M et al (2015) Diagnosis of sarcomatoid renal cell carcinoma with CT: evaluation by qualitative imaging features and texture analysis. AJR Am J Roentgenol 204: 1013–1023
53. Smith AD, Gray MR, del Campo SM et al (2015) Predicting overall survival in patients with metastatic melanoma on antiangiogenic therapy and RECIST stable disease on initial posttherapy images using CT texture analysis. AJR Am J Roentgenol 205:W283–W293
54. Takahashi N, Leng S, Kitajima K et al (2015) Small (< 4 cm) renal masses: differentiation of angiomyolipoma without visible fat from renal cell carcinoma using unenhanced and contrast-enhanced CT. AJR Am J Roentgenol 205:1194–1202
55. Ng F, Kozarski R, Ganeshan B, Goh V (2013) Assessment of tumor heterogeneity by CT texture analysis: can the largest cross-sectional area be used as an alternative to whole tumor analysis? Eur J Radiol 82:342–348
56. Cornejo KM, Dong F, Zhou AG et al (2015) Papillary renal cell carcinoma: correlation of tumor grade and histologic characteristics with clinical outcome. Hum Pathol 46:1411–1417
57. Sika-Paotonu D, Bethwaite PB, McCredie MR, William Jordan T, Delahunt B (2006) Nucleolar grade but not Fuhrman grade is applicable to papillary renal cell carcinoma. Am J Surg Pathol 30: 1091–1096